Research Square

Preprints are preliminary reports that have not undergone peer review.
They should not be considered conclusive, used to inform clinical practice,
or referenced by the media as validated information.

Reaction Pathway Engineering for Nitrate Production in Atmospheric-Pressure Plasma via an Alternative Organic Nitrogen Source

Yuan-Tai Lai
National Tsing-Hua University
Pin-Hao Huang
National Tsing-Hua University
Hori Masaru
Nagoya University
Jenq-Gong Duh
jgd@mx.nthu.edu.tw

National Tsing-Hua University

Research Article

Keywords: plasma-activated water, plasma treatment, organic fertilizer, nitrate production, waste recycling

Posted Date: September 30th, 2026

DOI: https://doi.org/10.21203/rs.3.rs-10902073/v1

License: This work is licensed under a Creative Commons Attribution 4.0 International License.
Read Full License

Additional Declarations: No competing interests reported.

Abstract

Plasma-activated water (PAW) has attracted attention for agricultural applications because plasma treatment can generate reactive oxygen and nitrogen species (RONS) and promote nitrate formation. However, increasing plasma power to enhance nitrate production also increases energy consumption, while the resulting nitrate increase may remain limited. In this study, plasma-activated coffee ground solutions (PAC) were prepared by introducing spent coffee grounds into deionized water treated at different plasma input powers. Nitrate production and the physicochemical properties of PAW and PAC were compared to evaluate the effects of plasma power and the presence of the organic species. Although increasing plasma power enhanced nitrate production in PAW, the increase was relatively limited. In contrast, the addition of spent coffee grounds substantially enhanced nitrate production under the same plasma conditions. Optical emission spectroscopy indicated prominent oxygen- and hydroxyl-related emissions, whereas nitrogen-related emissions were comparatively less pronounced, suggesting that reactive oxygen species (ROS) are more readily generated than reactive nitrogen species (RNS) under the present conditions. These results suggest that nitrate production can be enhanced by introducing an organic nitrogen source and utilizing plasma-generated reactive oxygen species, rather than relying solely on increased plasma power. This approach may reduce the need for additional plasma energy input while providing a potential route for the valorization and recycling of nitrogen-containing organic waste.

2. Introduction

The increasing global demand for food has intensified the need for efficient approaches to agricultural production and nitrogen management. The global food crisis is associated with limitations in food availability and increasing pressure on agricultural resources [1, 2]. Modern agriculture relies heavily on nitrogen fertilizers, while ammonia production through the Haber–Bosch process requires substantial energy input and is associated with environmental impacts [3, 4]. These challenges have stimulated interest in alternative approaches for nitrogen conversion and fertilizer production.

Composting is a well-established approach for recycling agricultural and organic waste and returning nutrients to soil. However, conventional composting can involve long processing times, relatively low nutrient availability, and odor generation [5]. The plasma-activated water (PAW) has emerged as a potential plasma-based approach for agricultural applications. It has been investigated for applications including pathogen control, seed germination [6], and fertilizer production [7]. However, the efficiency of nitrate formation in PAW strictly depends on plasma-induced nitrogen conversion. Although increasing plasma input power can enhance plasma reactions, higher power also results in greater energy consumption, and a proportional increase in nitrate production cannot necessarily be expected. Therefore, improving nitrate production solely by increasing plasma power might not represent the most effective approach, highlighting the need to explore alternative reaction pathways and nitrogen sources.

One potential strategy is to combine plasma treatment with nitrogen-containing organic materials [8]. Recent studies have investigated the use of plasma-treated organic materials for fertilizer-related applications, demonstrating the potential of plasma-generated reactive species to promote nitrogen conversion [9]. Spent coffee grounds are an abundant organic waste material generated from the widely consumed coffee industry [10] and contain nitrogen-containing components [11], making them a potential material for plasma-assisted nitrogen conversion. Their incorporation into PAW therefore provides an opportunity to investigate whether an organic nitrogen source can enhance nitrate production under plasma treatment, while simultaneously utilizing an organic waste resource.

In this study, plasma-activated coffee ground solutions (PAC) were prepared by introducing spent coffee grounds into PAW treated at different plasma input powers. Nitrate production and the physicochemical properties of PAW and PAC were investigated to evaluate the effects of plasma power and the presence of the organic nitrogen. Optical emission spectroscopy (OES) was employed to characterize the reactive species generated during plasma treatment. The relationship between plasma conditions, reactive species generation, and nitrate production was further examined to clarify the factors governing nitrate formation in PAW and PAC. This approach provides a basis for evaluating whether modifying the nitrogen source and reaction pathway can improve nitrate production without relying solely on increased plasma power.

3. Materials and Methods

3.1 Preparation for Plasma-Activated Water (PAW) and Plasma-Activated Coffee Ground Solution (PAC)

The experimental setup of the atmospheric-pressure plasma jet (APPJ) is illustrated in Fig. 1. The plasma source consisted of a tungsten high-voltage electrode positioned inside a quartz tube, while a copper plate placed beneath the sample beaker served as the grounded electrode. Compressed air was employed as the working gas at a flow rate of 10 standard liters per minute (SLM), which was regulated using a mass flow controller (MFC). The plasma was generated using a DC-pulse power supply (SPIK-2000A, Shenchang Electric Co., Ltd., Taiwan). Three operating powers were investigated: 80 W (40 kV, 20 mA), 130 W (44 kV, 30 mA), and 180 W (48 kV, 37.5 mA).

Plasma-activated water (PAW) was prepared by directly exposing 100 mL of deionized (DI) water to the APPJ for 10 min under each operating condition. In this study, plasma-activated coffee-ground solution (PAC) refers to the suspension obtained by directly treating the spent coffee-ground/DI-water mixture with APPJ, without prior filtration or separation of the solid residue. For plasma-activated coffee-ground solution (PAC), 3 g of spent coffee grounds were first dispersed in 100 mL of DI water and allowed to stand for 1 h at room temperature to facilitate the dissolution of water-soluble components. The resulting suspension was then directly treated by the APPJ for 10 min under identical plasma conditions. Throughout the study, the presence of spent coffee grounds was the primary difference between the

PAW and PAC treatments, while the plasma operating parameters, gas flow rate, treatment volume, and treatment time were kept identical for direct comparison.

3.2 Characterization of PAW and PAC

Optical emission spectroscopy (OES; USB2000+, Ocean Optics, USA) was employed to monitor the optical emission of the APPJ during plasma discharge. The emission spectra were used to identify the plasma-generated reactive species and to compare the relative emission characteristics under different plasma powers. No absolute species concentration was derived from the OES measurements. Each experimental condition was conducted using the same plasma treatment time and gas flow rate to ensure consistent comparison between PAW and PAC.

The physicochemical properties of PAW and PAC were characterized immediately after plasma treatment. The oxidation–reduction potential (ORP) was determined using an ORP meter (PH200 Ion Versatile Water Analysis Meter, CLEAN Instrument, China). The nitrate concentration was determined using an ion-selective electrode (9707BNWP, Thermo Scientific, USA). All measurements were performed at room temperature.

4. Results and Discussion

4.1 Nitrate production under different plasma powers

Nitrate (NO_3^-) is one of the major long-lived reactive nitrogen species generated in plasma-activated water and serves as an important nitrogen source for agricultural applications. Figure 2 compares the nitrate concentrations obtained in conventional plasma-activated water (PAW) and plasma-activated coffee-ground solution (PAC) under plasma powers of 80, 130, and 180 W.

For PAW, the nitrate concentration increased progressively with increasing plasma power, indicating that higher discharge power promoted nitrate formation under the present experimental conditions. This trend is consistent with previous studies reporting that higher discharge power generally enhances the generation of plasma reactive species, thereby promoting nitrate formation in the liquid phase [12]. However, the increases were quite limited. A similar increasing trend was observed for PAC. The untreated coffee-ground suspension exhibited a background nitrate concentration of 4.2 ppm prior to plasma treatment. However, at every plasma power investigated, PAC consistently produced substantially higher nitrate concentrations than PAW. More importantly, the increase associated with the presence of coffee grounds was considerably greater than that achieved by increasing the plasma power alone. For instance, PAC at only 80 W produced a nitrate concentration of 56.1 ppm, which already exceeded that of PAW at 180 W (51.1 ppm).

The enhanced nitrate production observed in PACS suggests that the presence of dissolved organic components plays an important role during plasma treatment. Since all plasma operating parameters were kept identical for PAW and PAC, the observed difference cannot be attributed solely to the electrical

energy supplied to the discharge. Instead, the results imply that additional chemical processes associated with the liquid composition contribute to nitrate formation. To elucidate this behavior, the plasma characteristics and the possible nitrate formation mechanisms are discussed in the following sections.

4.2 Plasma Characteristics and Solution Redox Properties

4.2.1 Optical Emission Spectroscopy (OES)

This study utilizes Optical Emission Spectroscopy (OES) to analyze the composition of active species within air atmospheric pressure plasma jets (APPJ) operating at various power levels. Figure 3 illustrates the OES spectra of the APPJ at 80 W, 130 W, and 180 W. It is evident that the composition of the active species within the atmospheric plasma remains highly consistent across different power outputs. Utilizing air as the working gas, hydroxyl radicals (OH) and the nitrogen second positive system represent the primary emitting components of the plasma jet.

Because the plasma-liquid interface was open to the atmospheric environment, hydroxyl radicals (OH) and hydrogen radicals (H) were generated via the electron-impact dissociation of water molecules, as evidenced by the distinct OH emission peak at 310 nm [13]. Furthermore, the Hα emission line at 656.2 nm [14] indicates that dissociated hydrogen atoms were excited to higher energy levels by energetic electrons, emitting at this specific wavelength upon relaxation to a lower energy state.

The majority of the identified nitrogen-related species emit in the wavelength range of 330 to 430 nm. These observed peaks predominantly correspond to the nitrogen second positive system, originating from the excitation of the air working gas, wherein energy is transferred to ambient nitrogen, allowing a minute fraction to be excited by the plasma [15]. Additionally, a distinctive emission at 391.4 nm corresponds to the N_2^+ (B-X) first negative system (FNS), which is attributed to the Penning effect [16]. Since the feed gas contains oxygen directed toward the high-energy discharge zone, excited atomic oxygen could be clearly detected in the spectrum at 777 nm and 844 nm [17, 18]. The NO radical, which serves as a crucial precursor for nitrite and nitrate, was located at 296 nm [19]. This species is formed through the combination of nitrogen and oxygen molecules [20]. However, the NO radical exhibited relatively weak intensity in the spectrum, largely owing to its short-lived nature.

Notably, while the overall emission intensity scales with increasing applied power, the relative intensity ratios among the various species (e.g., the ratio of N_2 SPS to OH or O) remain largely consistent across 80W, 130W, and 180W. In plasma physics, the relative intensity ratios among the major emission features remain broadly similar at 80, 130, and 180 W. This spectral consistency suggests that increasing the applied power does not substantially alter the dominant excitation characteristics of the discharge. Rather, the increased power may primarily increase the overall electron population without substantially changing the characteristic electron-energy distribution.

It is crucial to distinguish between molecular excitation and molecular dissociation. Although intense N_2 (SPS) emission peaks are observed, these primarily represent molecular excitation events. The dissociation of the strong N_2 triple bond (requiring ~ 9.8 eV [21]) is necessary to form reactive nitrogen atoms for subsequent NO generation. The relatively weak NO emission observed at 296 nm, contrasted with the prominent ROS (OH, O) signals, implies a chemical bottleneck. This indicates that the relatively weak NO emission, together with the strong O and OH emission features after dissociation (energy thresholds around 5–6 eV [22] and 6.5–7 eV [23]), suggests that the formation of reactive oxygen species may be more favorable than efficient N_2 dissociation under the present plasma conditions. This possibility is examined further using electron-impact dissociation cross sections and a conceptual EEDF in Section 4.3.

4.2.2 Oxidation-Reduction Potential (ORP)

Oxidation-reduction potential (ORP) measurements were utilized to examine the oxidizing capability of PAW and PAC under various power conditions. The ORP reflects the ability of a solution to oxidize or reduce another substance, depending fundamentally upon the concentration and strength of dissolved oxidizers [24]. Previous studies have reported that a higher ORP value is directly correlated with the generation and dissolution of plasma-induced active species, such as H_2O_2, nitric acid, and nitrous acid [25].

The ORP values of PAW and PAC are presented in Fig. 4. For PAW, the solution exhibited high ORP values after plasma treatment due to the dissolution of additional ROS into the deionized water. However, analysis of Fig. 4 reveals that the ORP values for PAW remain relatively similar across different power levels. The relatively small variation in ORP with increasing plasma power suggests that the overall redox state of PAW changes only marginally under the present treatment conditions. This behavior would reflect a equilibrium among plasma generation, dissolution, and subsequent consumption of reactive species in the liquid phase. Consequently, further increasing the plasma power fails to significantly elevate the solubility of these reactive species in the liquid phase. This solubility limitation perfectly corroborates the results shown in Fig. 2, explaining why the nitrate concentration in PAW exhibits only a marginal increase with higher power. The macroscopic ORP trends and the PAW nitrate concentrations mutually validate each other.

On the other hand, when comparing PAW and PAC at 80 W, the ORP of PAC exhibits a dramatic decrease. This substantial reduction occurs primarily because the dissolved ROS in the PAC system is consistent with the consumption of plasma-generated oxidizing species by dissolved organic constituents during the plasma treatment. As proven by previous research, the amino acids released from the coffee grounds in PAC readily react with these dissolved ROS to ultimately produce NO_3^- [26]. Therefore, the lower ORP of PACS is consistent with consumption of plasma-generated oxidizing capacity by dissolved organic constituents during treatment.

It is noteworthy that although the initial addition of coffee grounds lowers the ORP due to the rapid consumption of ROS by organic nitrogen, increasing the plasma input power (to 130 W and 180 W) for the PAC system continuously injects additional ROS into the solution. Under these higher power conditions, the continuous supply of ROS surpasses the immediate consumption rate by the dissolved organics. This mass-balance dynamic leads to a concurrent recovery in the ORP of the PAC alongside a significant, proportional boost in NO_3^- concentration. Ultimately, while the OES spectra reveal the inherent abundance of ROS generation in the gas phase, the ORP trends provide critical liquid-phase evidence, implying that ROS are continuously transferred into the liquid and actively maintain their reactivity, rather than reaching a non-productive saturation limit as observed in PAW. These abundant ROS are effectively captured and utilized to drive the oxidation of organic nitrogen.

4.3 Conceptual Electron Energy Distribution Function (EEDF) analysis

4.3.1 Relationship between Electron Energy and Plasma Reactions

According to OES results, dissociation and excitation are major electron-impact processes under the present APPJ conditions. However, excitation alone is unlikely to be the dominant process governing nitrate formation. During plasma discharge, electron-impact reactions dissociate nitrogen-, oxygen-, and water-containing molecules, generating reactive nitrogen and oxygen species (RNS and ROS). These reactive species subsequently undergo a series of gas-phase and plasma–liquid interfacial reactions, leading to the formation of nitrite and ultimately nitrate in the liquid phase. Since each electron-impact process requires a minimum electron energy to occur, the reaction probability depends on whether the electron energy exceeds the corresponding threshold energy. The relationship between Electron Energy and Reaction is organized in Table 1. The threshold energy represents the minimum electron energy required for dissociation process to occur. The peak cross-section energy refers to the electron energy corresponding to the maximum collision cross section, where the probability of the electron-impact reaction is greatest. Electrons with energies near the peak cross-section energy contribute most effectively to the corresponding electron-impact process, whereas electrons with energies above the threshold energy may also participate with lower probabilities.

Table 1
The Threshold Energy and Peak Cross Section Energy of the reactions

Molecule dissociation	Reaction	Threshold Energy (eV)	Peak Cross Section Energy (eV)
O_2	$O_2 + e^- \rightarrow 2\,O$	5–6	12–15 [20]
H_2O	$H_2O + e^- \rightarrow OH$	6.5 -7	15–20 [21]
N_2	$N_2 + e^- \rightarrow 2\,N$	9.8	80–100 [27]

4.3.2 Combination of the EEDF and electron-impact cross sections

The Electron Energy Distribution Function (EEDF) fundamentally represents the probability density of electron kinetic energies within the plasma, dictating the fraction of electrons capable of overcoming specific reaction thresholds. In this study, the EEDF profiles (Fig. 5) are presented as conceptual representations of electron-energy distributions in a non-equilibrium atmospheric-pressure plasma. The profiles are not experimentally measured or numerically calculated EEDFs, but are used solely to qualitatively illustrate the energy ranges in which different electron-impact dissociation processes may occur. The conceptual profiles are used to compare their qualitative overlap with the electron-impact dissociation cross sections of O_2, H_2O, and N_2.

As the applied input power increases from 80 to 180 W, the conceptual profiles are used to represent an increase in the population of electrons contributing to the discharge, while the overall distribution is assumed to retain a similar characteristic shape. However, the shape of the distribution does not shift significantly toward the high-energy regime. This behavior is intrinsically linked to the physical nature of atmospheric-pressure discharges, the extremely high collision frequency between electrons and heavy neutral gas molecules rapidly dissipates electron kinetic energy. Consequently, simply increasing the macroscopic power primarily generates more electrons rather than substantially raising the average electron energy.

To comprehensively evaluate the dominant plasma-chemical reactions, the macroscopic reaction rate can be fundamentally understood as the convolution of the EEDF and the energy-dependent electron-impact dissociation cross-section ($\sigma\ (E)$), as seen in Fig. 5. The dissociation cross-sections for O_2, H_2O, and N_2 utilized in this conceptual overlay are based on established literature values as summarized in Table 1. By superimposing the conceptual EEDF with these dissociation cross-sections, the effective reaction windows can be qualitatively visualized, which are represented by the shaded overlap areas in the figure. As illustrated, the bulk region of the EEDF substantially overlaps with the dissociation cross-sections of O_2 and H_2O. Conversely, the relatively high threshold energy for electron-impact dissociation of N_2 lies predominantly within the rapidly decaying high-energy tail of the conceptual EEDF, resulting in a distinctly minimal overlap area. In conventional PAW, atmospheric N_2 serves as the absolute sole

nitrogen source; thus, this specific, minimal overlap region represents the only effective electron energy window capable of initiating nitrate production.

This physical superimposition visually and theoretically confirms that the current plasma system inherently favors the dissociation of O_2 and H_2O to generate an abundant amount reactive oxygen species (ROS). Meanwhile, the generation of reactive nitrogen species (RNS) and consequently the final nitrate yield in conventional PAW remains severely constrained by the limited electron population within that narrow, high-energy overlap area. Because overcoming this N_2 dissociation bottleneck via simple power increments is fundamentally inefficient, the plasma system intrinsically produces a highly ROS-rich environment. This physical constraint indicates that improving the overall conversion efficiency requires a strategic shift rather than attempting to force RNS generation against the EEDF limitation, and the excessive and energetically favorable ROS must be effectively harnessed. This sets the theoretical foundation for an alternative reaction pathway.

4.4 Alternative nitrate pathways

As demonstrated in the preceding sections, increasing the applied plasma power produced only a limited increase in nitrate concentration in PAW, whereas a substantially larger increase was observed in PAC. The OES results and conceptual EEDF analysis suggest that the current APPJ conditions favor the generation of reactive oxygen species (ROS), while the formation of reactive nitrogen species (RNS) through N_2 dissociation is comparatively constrained. This difference suggests that nitrate formation in PAW is primarily governed by the availability of plasma-generated RNS and that simply increasing plasma power might not efficiently overcome this limitation.

In conventional PAW, atmospheric N_2 is the primary nitrogen source for nitrate formation. Electron-impact dissociation of N_2 requires relatively high electron energies because of its strong triple bond. Under the present APPJ conditions, only a limited fraction of electrons can effectively contribute to this process, restricting the formation of nitrogen-derived reactive species. In addition, nitrogen oxide intermediates formed in the gas phase, such as NO and NO_2, have relatively low solubility in water. Their transfer from the gas phase into the liquid phase can therefore represent an additional limitation for subsequent aqueous-phase conversion toward nitrate. Consequently, the conventional pathway can be described conceptually as an **RNS-controlled pathway**, in which both nitrogen activation and subsequent gas–liquid transfer of nitrogen-containing intermediates influence the overall nitrate production efficiency.

The PAC system provides a different reaction environment by introducing nitrogen-containing organic compounds from the spent coffee grounds. Unlike atmospheric N_2, many organic nitrogen compounds, including amino acids, are readily soluble or dispersible in water and can therefore be present directly in the liquid phase during plasma treatment. This reduces the dependence on gas-phase N_2 activation and the subsequent transport of poorly soluble nitrogen oxide intermediates from the plasma region into the liquid. Furthermore, organic nitrogen compounds contain chemical bonds that can be more readily

attacked by strong oxidizing species than the N ≡ N bond of molecular nitrogen. They can therefore provide accessible materials for reactions with the abundant ROS generated under the present APPJ conditions.

The proposed difference between the two pathways is illustrated schematically in Fig. 6. In PAW, nitrate formation follows predominantly an **RNS-mediated pathway**, in which atmospheric N_2 must first be activated to nitrogen-containing reactive intermediates before subsequent conversion to nitrate in the aqueous phase. The limited availability of sufficiently energetic electrons for N_2 dissociation, together with the relatively low aqueous solubility of NO and NO_2, can restrict the efficiency of this pathway. In PAC, organic nitrogen provides an additional nitrogen source that is already associated with the liquid phase. These dissolved nitrogen-containing compounds can interact more directly with plasma-generated ROS, providing an alternative route toward oxidized nitrogen species and ultimately nitrate.

This interpretation is also consistent with the ORP behavior observed in PAC. The markedly lower ORP of PAC at the lowest plasma power compared with PAW indicates that the oxidizing capacity introduced into the liquid is affected by the presence of dissolved organic constituents. As the plasma power increases, additional ROS are supplied to the PAC system, accompanied by a substantial increase in nitrate concentration. These observations suggest that the organic substrate provides additional reaction sites for plasma-generated oxidizing species, allowing a greater fraction of the ROS generated by the plasma to participate in nitrogen conversion.

Therefore, the enhanced nitrate production in PAC should not be interpreted simply as the result of generating more plasma species by increasing power. Rather, the results support a **reaction-pathway engineering concept**, in which an additional, readily accessible organic nitrogen source is introduced to utilize the ROS that are preferentially generated under the current APPJ conditions. Such a pathway can partially bypass the energy-demanding N_2 activation step and reduce the dependence on increasing plasma power, while simultaneously providing a route for the valorization of nitrogen-containing organic waste

5. Conclusion

This study demonstrated that nitrate production in PAW cannot be effectively enhanced solely by increasing plasma input power under the present APPJ conditions. Although higher plasma power increased the nitrate concentration of PAW, the improvement was relatively limited. In contrast, the introduction of spent coffee grounds substantially enhanced nitrate production under comparable plasma conditions, indicating that the availability of an additional organic nitrogen source can strongly influence nitrate formation.

OES analysis showed prominent oxygen- and hydroxyl-related emissions, while nitrogen-related emissions were comparatively less pronounced. Together with the electron-impact reaction analysis, these observations suggest that reactive oxygen species are more readily generated than reactive nitrogen species under the present plasma conditions. The enhanced nitrate production observed in PAC

therefore supports an alternative reaction pathway in which plasma-generated reactive species participate in the conversion of organic nitrogen toward nitrate, rather than relying solely on increased plasma-driven nitrogen fixation.

These findings suggest that modifying the nitrogen source and reaction pathway may provide a means to reduce reliance on additional plasma energy input while simultaneously promoting the valorization of nitrogen-containing organic waste. Further development of this approach could provide an alternative strategy for plasma-assisted nitrate production and organic waste recycling.

Declarations

Competing Interests:

The authors declare that they have no competing interests.

Funding:

This study was supported by the National Science and Technology Council, Taiwan, under Grant No. NSTC 115-2221-E-007-009.

Author Contribution

Conceptualization: Yuan-Tai Lai, Jenq-Gong Duh; Methodology: Yuan-Tai Lai, Pin-Hao Huang; Investigation: Yuan-Tai Lai, Pin-Hao Huang; Formal analysis: Yuan-Tai Lai; Writing – original draft: Yuan-Tai Lai; Writing – review and editing: Jenq-Gong Duh, Hori Masaru; Supervision: Jenq-Gong Duh, Hori Masaru.

Acknowledgement

This study was financially supported by the National Science and Technology Council (NSTC), Taiwan, under Grant No. NSTC 115-2221-E-007-009.

Data Availability

The datasets generated during and/or analysed during the current study are available from the corresponding author on reasonable request.

References

1. Richmond P, Roehner BM, Wang QH (2019) The physics of large-scale food crises. Phys A 522:274–293
2. Pimental D (1976) World Food Crisis: Energy and Pests. Bull Entomol Soc Am 22:20–26
3. Ghavam S, Vahdati M, Wilson IAG, Styring P (2021) Sustainable ammonia production processes. Front Energy Res 9:580808
4. Glibert PM, Maranger R, Sobota DJ, Bouwman L (2014) The Haber Bosch–harmful algal bloom (HB–HAB) link. Environ Res Lett 9:105001
5. Ayilara MS, Olanrewaju OS, Babalola OO, Odeyemi O (2020) Waste management through composting: Challenges and potentials. Sustainability 12:4456
6. Randeniya LK, de Groot GJJB (2015) Non-Thermal Plasma Treatment of Agricultural Seeds for Stimulation of Germination, Removal of Surface Contamination and Other Benefits: A Review. Plasma Chem Plasma Process 12:608–623
7. Gromov M, Gorbanev Y, Vervloessem E, Morent R, Snyders R, De Geyter N, Bogaerts A, Nikiforov A (2025) Electrification of fertilizer production via plasma based nitrogen fixation: a tutorial on fundamentals. RSC Sustain 3:757–780
8. Graves DB, Bakken LB, Jensen MB, Ingels R (2019) Plasma Activated Organic Fertilizes. Plasma Chem Plasma Process 39:1–19
9. Ku TN, Hsu SY, Lai YT, Chang SY, Duh JG (2023) Plasma-treated soybean dregs solution with various gas mixtures. IEEE Trans Plasma Sci 51:437–443
10. Pujol D, Liu C, Fages J, Marty B, Chrusciel H et al (2013) The chemical composition of exhausted coffee waste. Ind Crops Prod 50:423–429
11. Mussatto SI, Machado EMS, Martins S, Teixeira JA (2011) Production, composition, and application of coffee and its industrial residues. Food Bioprocess Technol 4:661–672
12. Dhungana S, Chalise R, Singh AK, Khanal R, Baniya HB (2026) Effect of operating conditions on physicochemical properties of plasma activated water prepared from a low-cost gliding arc discharge system. Desalin Water Treat 326:101741
13. Oh JS, Szili EJ, Ogawa K, Short RD, Ito M, Furuta H, Hatta A (2018) UV-vis spectroscopy study of plasma-activated water: dependence of the chemical composition on plasma exposure time and treatment distance. Jpn J Appl Phys 57:0102B9
14. Vesel A, Kovac J, Primc G, Junkar I, Mozetic M (2016) Effect of H_2S plasma treatment on the surface modification of a polyethylene terephthalate surface. Materials 9:95
15. Vlad IE, Anghel SD (2017) Time stability of water activated by different on-liquid atmospheric pressure plasmas. J Electrostat 87:284–292
16. Park HS, Kim SJ, Joh HM, Chung TH, Bae SH, Leem SH (2010) Optical and electrical characterization of an atmospheric pressure microplasma jet with a capillary electrode. Phys Plasmas 17:033502
17. Mohamed AAH, Basher AH, Almarashi JQM, Ouf SA (2021) Susceptibility of Staphylococcus epidermidis to argon cold plasma jet by oxygen admixture. Appl Sci 11:3455

18. Brisset JL, Pawlat J (2016) Chemical effects of air plasma species on aqueous solutes in direct and delayed exposure modes: Discharge, post discharge and plasma activated water. Plasma Chem Plasma Process 36:355–381
19. Bolouki N, Kuan WH, Huang YY, Hsieh JH (2021) Characterizations of a plasma-water system generated by repetitive microsecond pulsed discharge with air, nitrogen, oxygen, and argon gases species. Appl Sci 11:6158
20. Adhikari B, Adhikari M, Ghimire B, Park G, Choi EH (2019) Cold atmospheric plasma-activated water irrigation induces defense hormone and gene expression in tomato seedlings. Sci Rep 9:1–15
21. Wang P, Gong S, Li Y, Mo Y (2024) Bond dissociation energy of N2 measured by state-to-state resolved threshold fragment yield spectra. J Chem Phys 160:014304
22. Itikawa Y (2009) Cross Sections for Electron Collisions with Oxygen Molecules. J Phys Chem Ref Data 38:1–20
23. Itikawa Y, Mason N (2005) Cross Sections for Electron Collisions with Water Molecules. J Phys Chem Ref Data 34:1–22
24. Thirumdas R, Kothakota A, Annapure U, Siliveru K, Blundell R, Gatt R, Valdramidis VP (2018) Plasma activated water (PAW): Chemistry, physico-chemical properties, applications in food and agriculture. Trends Food Sci Technol 77:21–31
25. Boehm D, Heslin C, Cullen PJ, Bourke P (2016) Cytotoxic and mutagenic potential of solutions exposed to cold atmospheric plasma. Sci Rep 6:1–14
26. Chan YC, Lai YT, Hsu SY, Chen PY, Duh JG (2023) Effects of plasma-activated water via different gas treatments on coffee ground decomposition. IEEE Trans Plasma Sci 51:2282–2289
27. Itikawa Y, Hayashi M, Ichimura A, Onda K, Sakimoto K, Takayanagi K, Nakamura M, Nishimura H, Takayanagi T (1986) Cross Sections for Collisions of Electrons and Photons with Nitrogen Molecules. J Phys Chem Ref Data 15:985–1010

Figures

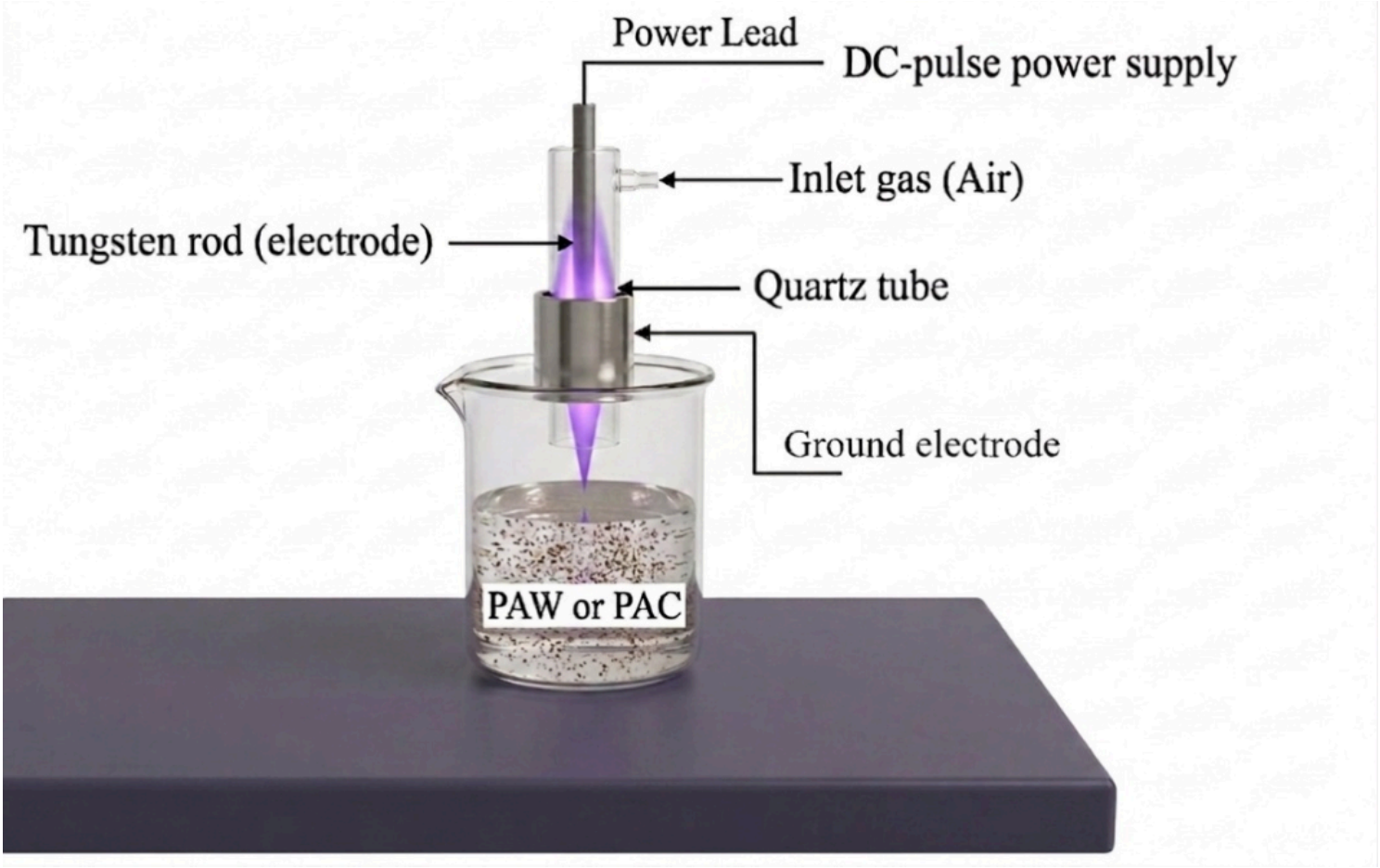


Figure 1

The experimental setup of an Atmospheric-pressure plasma jet (APPJ)

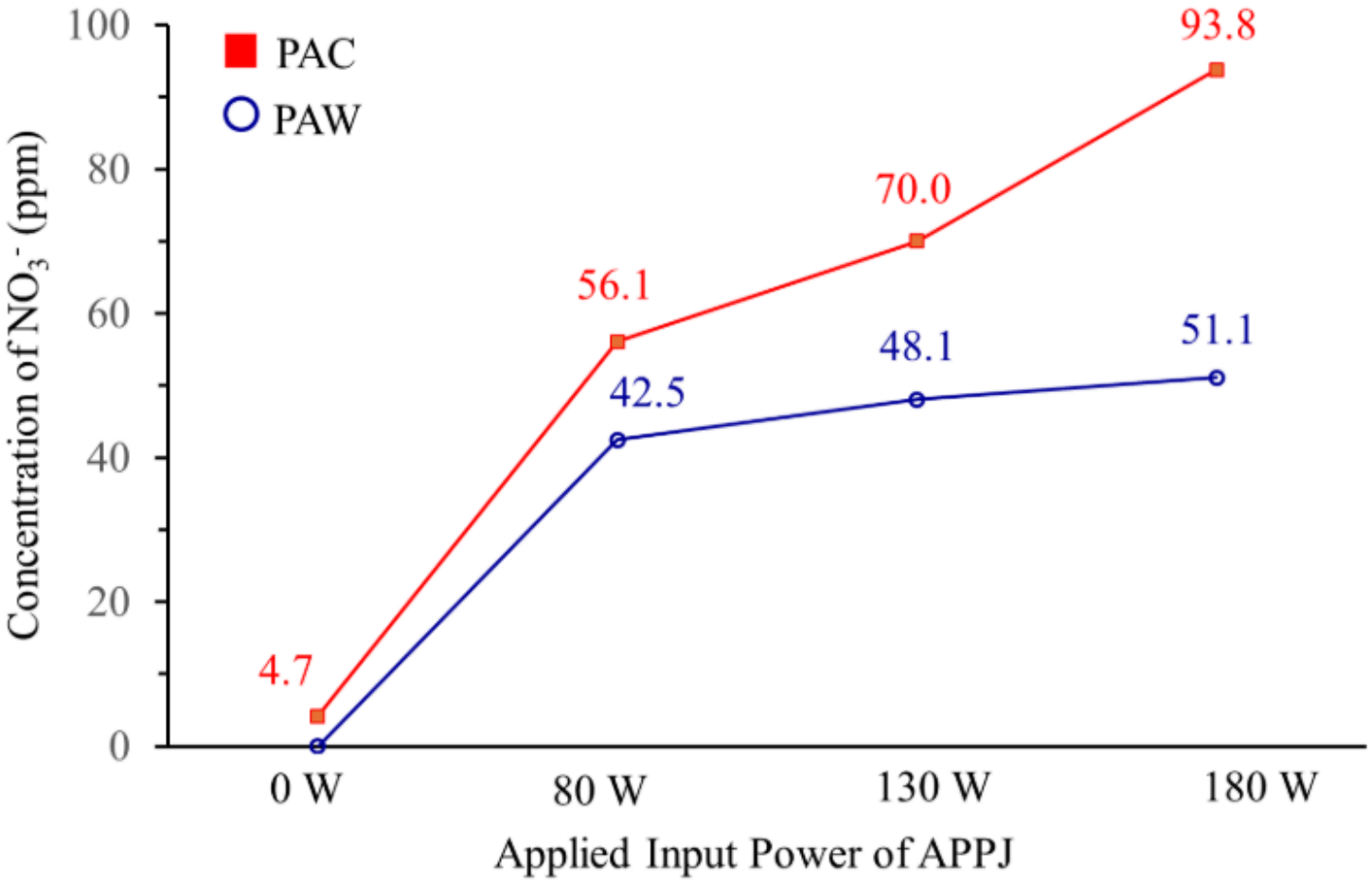


Figure 2

Nitrate concentration of PAW and PAC

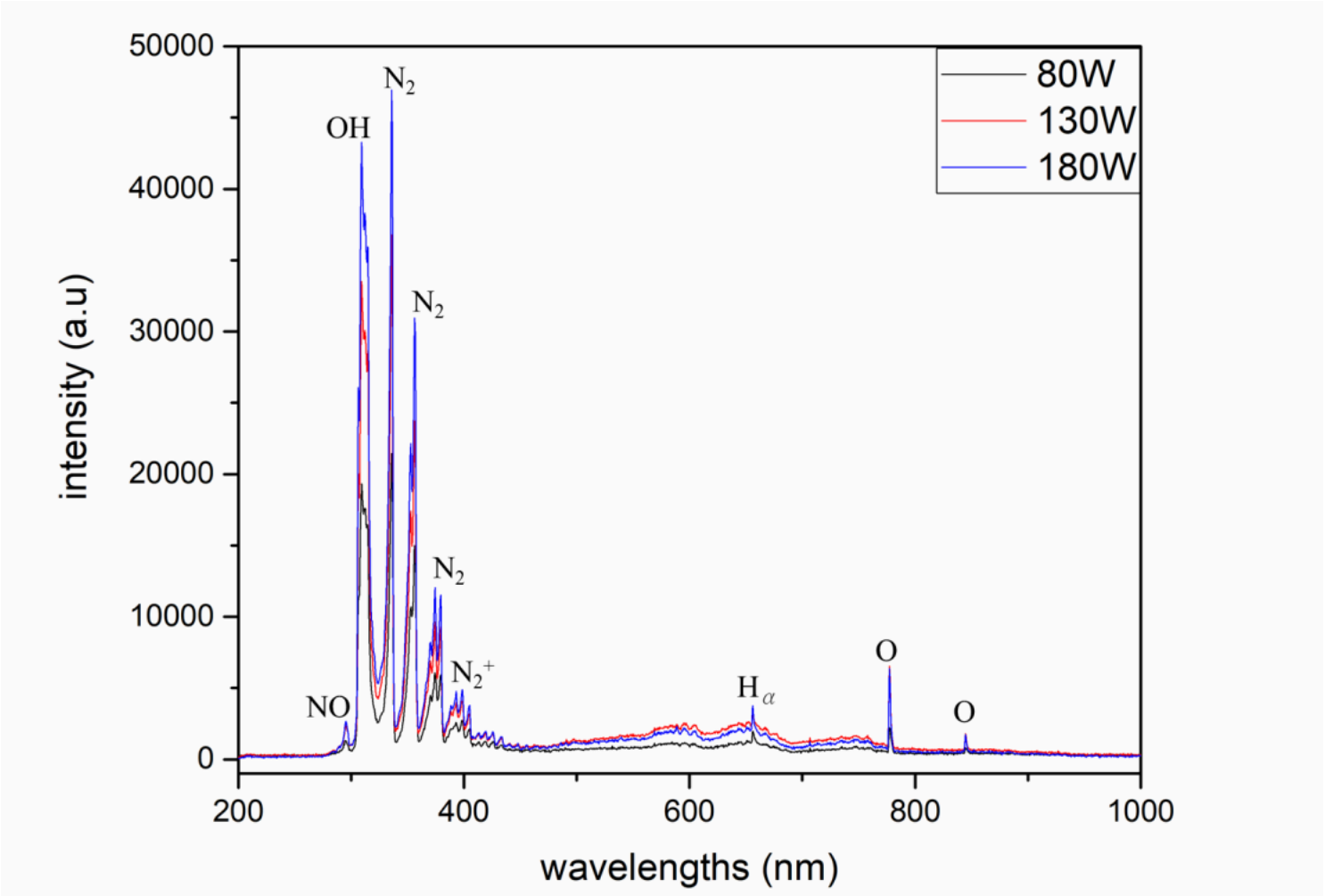


Figure 3

Optical Emission Spectrum (OES) of active species composition within air atmospheric plasma jets (APPJ) at raising power supplied

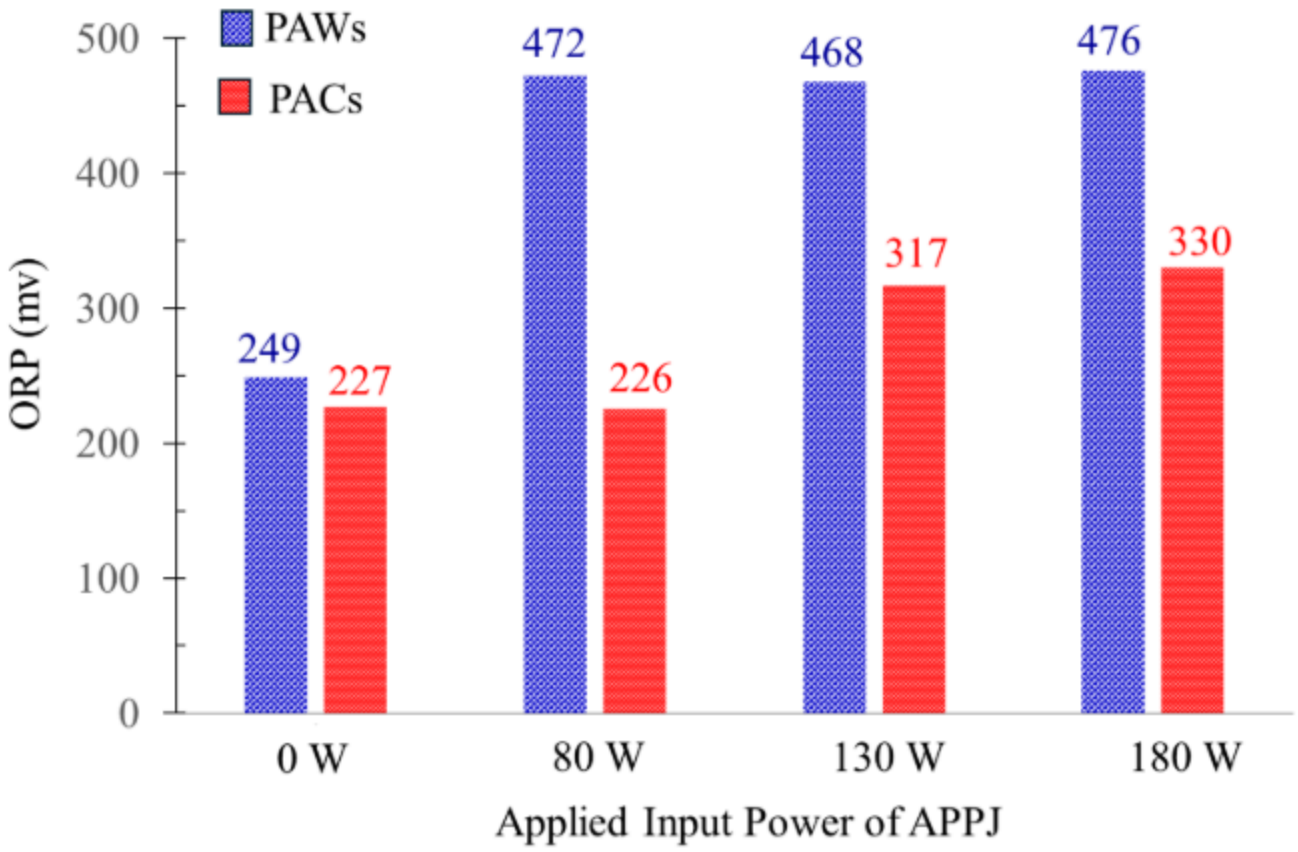


Figure 4

ORP value of PAW and PAC

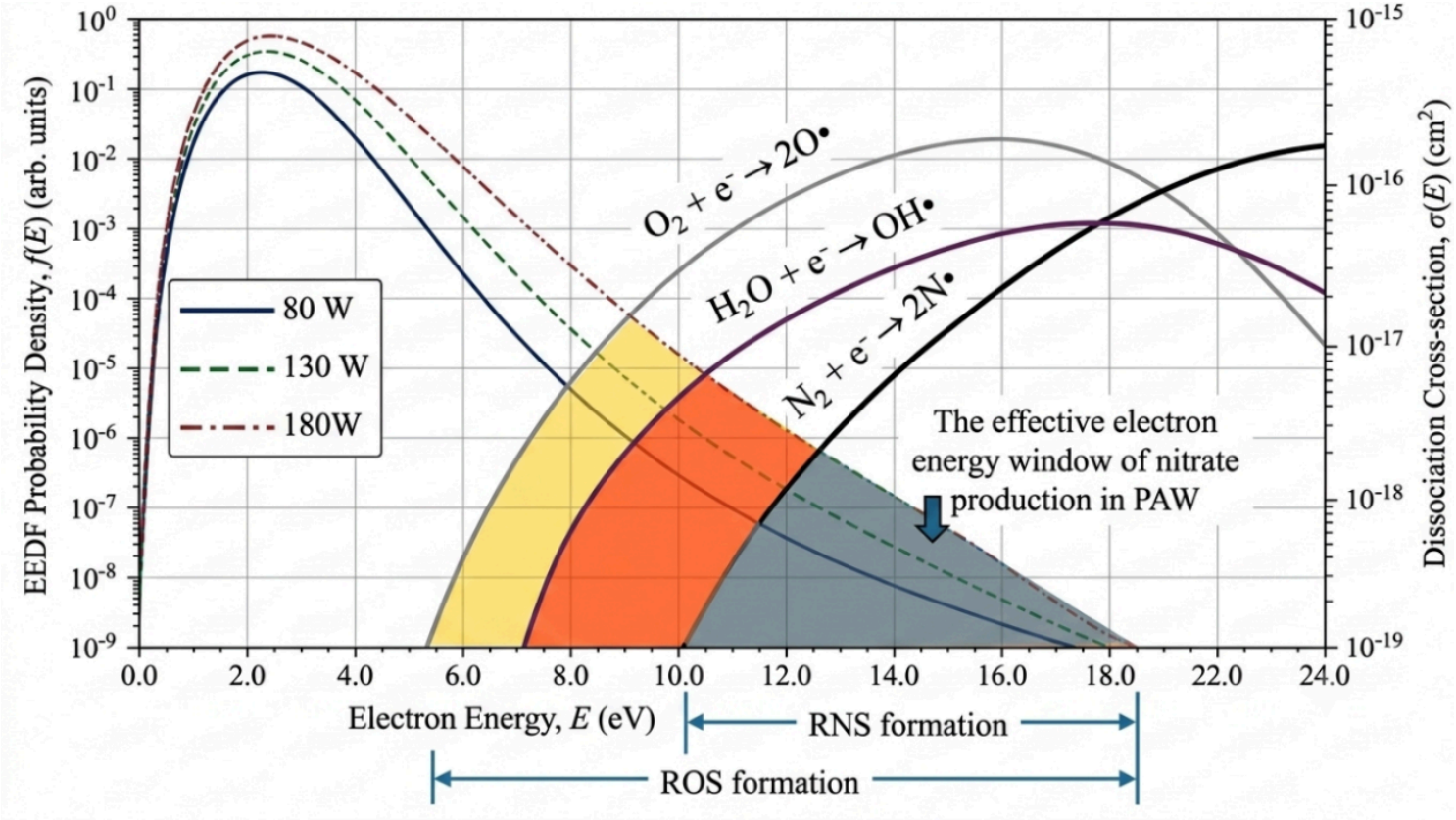


Figure 5

EEDF and electron-impact cross sections analysis

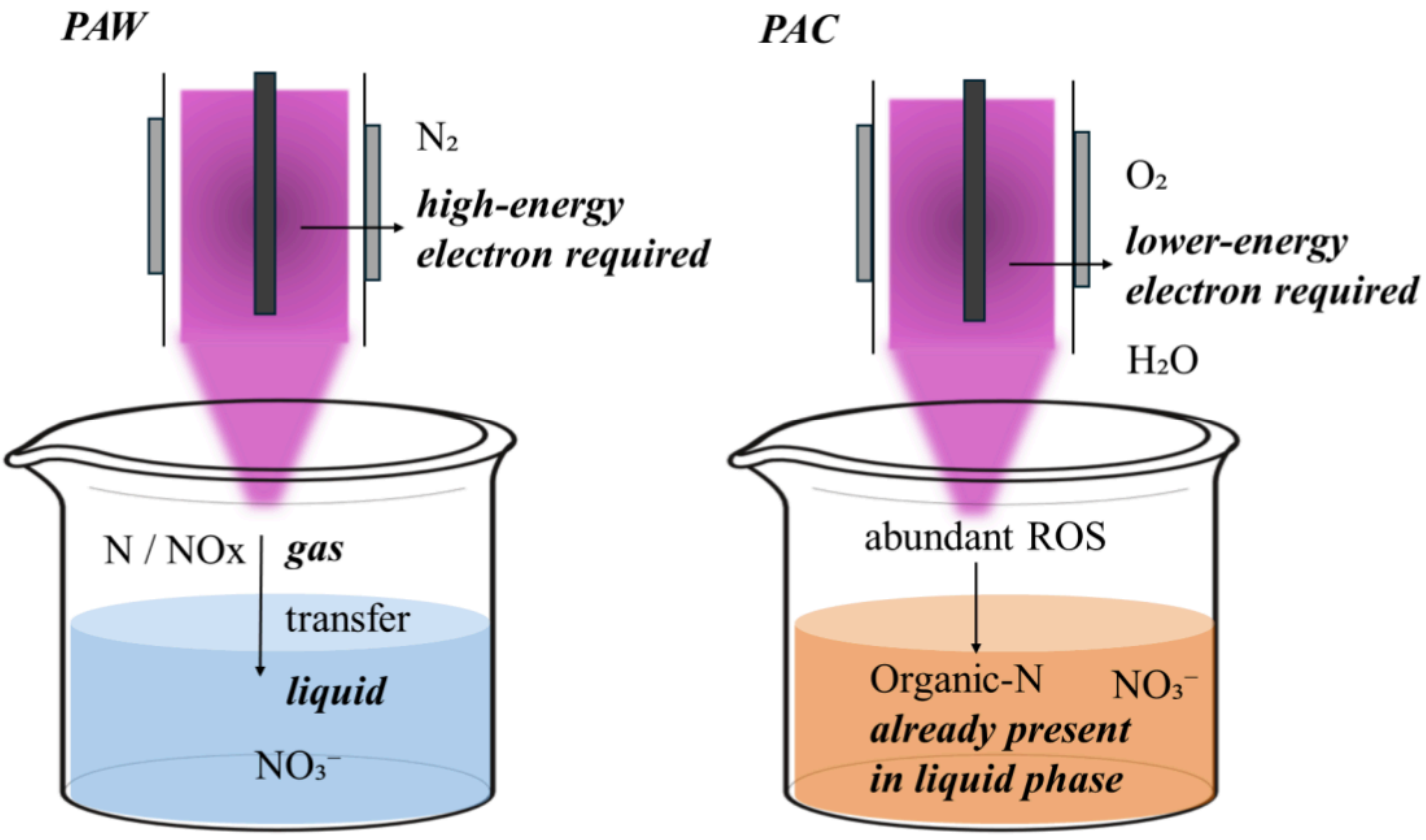


Figure 6

Alternative Nitrate Formation Pathway